Lipidomics analysis reveals new insights into the goose fatty liver formation

Rongxue Wei,[*,†] Rong Ning,[*,†] Chunchun Han ®[*,†,1] Shouhai Wei,[*,†] Yongqiang Teng,[*,†] Liang Li,[*,†] Hehe Liu,[*,†] Shengqiang Hu,[*,†] Bo Kang,[*,†] and Hengyong Xu[*,†]

[*]Key Laboratory of Livestock and Poultry Multi-omics, Ministry of Agriculture and Rural Affairs, College of Animal Science and Technology, Sichuan Agricultural University, Chengdu, Sichuan, 611130, PR China; and [†]Farm Animal Genetic Resources Exploration and Innovation Key Laboratory of Sichuan Province, Sichuan Agricultural University, Chengdu, Sichuan, 611130, PR China

ABSTRACT Our previous study described the mechanism of goose fatty liver formation from cell culture and transcriptome. However, how lipidome of goose liver response to overfeeding is unclear. In this study, we used the same batch of geese (control group and corn flour overfeeding group) to explore the lipidome changes and underlying metabolic mechanisms of goose fatty liver formation. Liquid chromatography-mass spectrometry (**LC-MS**) was provided to lipidome detection. Liver lipidomics profiles analysis was performed by principal component analysis (**PCA**), partial least squares-discriminant analysis (**PLS-DA**) and orthogonal partial least squares-discriminant analysis (**OPLS-DA**), different lipids were identified and annotated, and the enriched metabolic pathways were showed. The results of PCA, PLS-DA, and OPLS-DA displayed a clear separation and discrimination between control group and corn flour overfeeding group. Two hundred and fifty-one different lipids were yielded, which were involved in triglyceride (**TG**), diglyceride (**DG**), phosphatidic acids (**PA**), phosphatidylinositols (**PI**), phosphatidylethanolamines (**PE**), phosphatidylcholines (**PC**), lyso-phosphatidylcholines (**LPC**), monogalactosylmonoacylglycerol (**MGMG**), sphingolipids (**SM**), ceramides (**Cer**), and hexaglycosylceramides (**Hex1Cer**). Different lipids were enriched in glycerophospholipid metabolism, glycerolipid metabolism, phosphatidylinositol signaling system, inositol phosphate metabolism, glycosylphosphatidylinositol (**GPI**)-anchor biosynthesis and sphingolipid metabolism. In conclusion, this is the first report describing the goose fatty liver formation from lipidomics, this study might provide some insights into the underlying glucolipid metabolism disorders in the process of fatty liver formation.

Key words: goose fatty liver, lipidome, overfeeding, lipid accumulation, hepatic steatosis tolerance

INTRODUCTION

With the continuous advancement of biological technology, a substantial progress has been made in the study on the formation mechanism of fatty liver in goose from the physiological level to the genome and transcriptome level. It is generally considered that the formation of fatty liver in goose is primarily due to the imbalance between lipids synthesis, transport and fatty acids β-oxidation in the liver, which leads to excessive lipids deposition in the liver and promotes hepatocytes proliferation. This process is closely associated with endoplasmic reticulum stress, insulin resistance (**IR**) as well as hepatocyte growth and proliferation (Geng et al., 2015; Geng et al., 2016b; Wei et al., 2022b). A recent study suggests that the large amount of fat stored in goose liver results from an imbalance between the storage and secretion of exogenous and de novo synthesized endogenous lipids, as well as an absence of leptin gene homologs due to positive selection (Lu et al., 2015). As the goose liver capacity for and tolerance to severe hepatic steatosis, gut microbiota, adiponectin and liver fatty acids composition play important role. In overfed goose, complement system was suppressed due to the increasing levels of blood lactic acid produced by the enriched *Lactobacillus*, and TNFα was suppressed by the lactic acid via HNF1α/C5 pathway (Liu et al., 2016b). Adiponectin and its receptor have anti-inflammatory, insulin sensitization and anti-apoptotic effects in goose fatty liver formation (Geng et al., 2016a). Unsaturated fatty acids (**UFA**) could inhibit saturated fatty acids (**SFA**)-induced elevation of ceramides and inflammation, the level of UFA increased significantly after overfeeding,

specially (n-3) polyunsaturated fatty acids (Wei et al., 2022a). However, in the process of goose fatty liver formation, the changes of liver lipidomics profiles have not been elucidated.

Non-alcoholic fatty liver disease (**NAFLD**) is a metabolic dysfunction histologically characterized by hepatic fat accumulation (hepatic steatosis) in the absence of heavy alcohol consumption. Lipidomics, as a widely used analytical technique to analyze lipid metabolism, is helpful to search for NAFLD-related biomarkers (Vvedenskaya et al., 2021). Numerous liver diseases have been found to cause changes in plasma lyso-phosphatidylcholines (**LPC**) levels, making LPC a potential biomarker for NAFLD (Akerele and Cheema, 2015; Zhu et al., 2022). The ratio of phosphatidylcholines (**PC**) to phosphatidylethanolamines (**PE**) is a determinant of cell membrane integrity and a predictor of NAFLD (Li et al., 2006). Goose has an excellent capacity to accumulated lipid in liver. There are many similarities between goose fatty liver and nonalcoholic fatty liver. Thereby, not only can goose be used as a model organism, and also goose fatty liver can be treated as a unique model of hepatic steatosis for studying NAFLD. Overfed geese were fed a regular diet within a 20-d period of recovery, and the migratory bird after energy consumption of stored lipids, their liver was restored to the original state, and the entire process was reversible and caused neither cirrhosis nor necrosis in the liver (Davail et al., 2000; Xia et al., 2016). It suggested that waterfowl has developed a mechanism to protect its liver from the harms caused by severe hepatic steatosis in the process of adaptation. Autophagy can inhibit inflammation, and PE mediated the autophagy pathway (Song et al., 2019). However, whether these lipids mediated anti-inflammation or not is unclear during goose fatty liver formation.

Our previous study had confirmed overfeeding induced lipid accumulation in goose fatty liver; serum parameter detection showed that the level of glucose, triglyceride (**TG**), total cholesterol (**T-CHO**), very low-density lipoprotein (**VLDL**) and very high-density lipoprotein (**VHDL**) significantly after overfeeding (control group vs. corn flour overfeeding group); liver transcriptome analysis shown that the highest enrichment signal pathways related to differentially expressed genes (**DEGs**) (control group *vs* corn flour overfeeding group) in fatty acid metabolism, unsaturated fatty acid synthesis (biosynthesis of unsaturated fatty acids), peroxisome, steroid biosynthesis, and fatty acid elongation; liver fatty acids composition comparison also shown that the content and proportion of unsaturated fatty acids significantly increased after overfeeding with corn flour (Wei et al., 2022a). In this study, the same batch of geese (control group and corn flour overfeeding group) was used to investigate the changes in the lipidome, identify the potential biomarkers and metabolic pathways and reveal underlying metabolic mechanism of goose fatty liver formation. It will provide not only another possible perspective in further researching mechanism of goose

fatty liver formation, but also some theoretical basis for the diagnosis and treatment of NAFLD.

METHODS AND MATERIALS

Ethics Statement

All procedures in the present study were subject to approval by the Institutional Animal Care and Use Committee (**IACUC**) of Sichuan Agricultural University (Permit No. DKY-B20141401), and carried out in accordance with the approved guidelines. All efforts were made to minimize the suffering of the animals.

Sample Collection

In this study, the liver samples came from the same batch of geese (control group and corn flour overfeeding group) which came from previous study (Wei et al.,2022a). The overfeeding procedure and sampling were performed as this previously study. In brief, forty 13-wk-old male Tianfu Meat Geese which came from Experimental Farm for Waterfowl Breeding at Sichuan Agricultural University (Ya'an, China), were randomly divided into control groups and corn flour overfeeding group on average. All the experimental geese were reared in cages with a density of 3 birds /m^2, the temperature was controlled at about 25°, and light was provided at night. Birds had free access to water at all times. The geese of control group were normally fed with raw (uncooked) corn flour (ad libitum). The geese of corn flour overfeeding group were overfed with corn flour. Overfeeding lasted 3 wk. During overfeeding, the daily feed intake gradually increased. The daily feed intake reached 1,600 g corn flour (4 meals a day; corn flour: water = 1:0.75) on the 6th day. The feed formula of the diet for experiment was provided in Supplement materials 2: Table S1. After 12 h of fasting, 6 ganders of each group were anesthetized with intraperitoneal injection of sodium pentobarbital (60 mg/kg), and then killed; the liver was collected immediately for determination of liver lipidome.

Determination of Liver Lipidome

Six liver samples which came from control group and 6 liver samples which came from treatment group were provided to lipidome detection. Lipid extraction was performed as below. (1) transferred 100 mg of each sample into 2 mL centrifuge tubes, added 750 μL of chloroform methanol mixed solution (2:1) (precooled at $-20°C$) and 2 steel balls (The insufficient sample size is reduced to an equal scale); (2) ground the samples by a high flux organization grinding apparatus for 60 s at 60 Hz; (3) put samples on the ice for 40 min, added 190 μL L ddH2O and vortex mixed for 30 s, and still put on the ice for 10 min; (4) centrifuged the samples at 12,000 rpm for 5 min at room temperature and

transferred 300 μL lower layer fluid into a new centrifuge tube; (5) added 500 μL of chloroform methanol mixed solution (2:1) (precooled at -20°C) and vortex mixed for 30 s; (6) centrifuged the samples at 12,000 rpm for 5 min at room temperature and transferred 400 μL lower layer fluid into the same centrifuge tube above. Samples were concentrated to dry in vacuum; (7) samples were dissolved with 200 μL isopropanol, and the supernatant was filtered through 0.22 μm membrane to obtain the prepared samples for LC-MS; (8) take 20 μL from each sample to the quality control (QC) samples (these QC samples were used to monitor deviations of the analytical results from these pool mixtures and compare them to the errors caused by the analytical instrument itself); (9) the rest of the samples were used for liquid chromatography-mass spectrometry (LC-MS) detection.

Chromatographic separation was accomplished in an Thermo Vanquish system equipped with an ACQUITY UPLC BEH C18 (100 × 2.1 mm, 1.7 μm, Waters) column maintained at 50°C. The temperature of the autosampler was 8°C. Gradient elution of analytes was carried out with acetonitrile: water = 60:40 (0.1% formic acid +10 mM ammonium formate) (A2) and isopropanol: acetonitrile = 90:10 (0.1% formic acid +10 mM ammonium formate) (B2) at a flow rate of 0.25 mL/min. Injection of 2 μL of each sample was done after equilibration. An increasing linear gradient of solvent A (v/v) was used as follows: 0 to 5 min, 70 to 57% A2; 5 to 5.1 min, 57% to 50% A2; 5.1 to 14 min, 50% to 30% A2; 14 to 14.1 min, 30% A2; 14.1 to 21 min, 30% to 1% A2; 21 to 24 min, 1% A2; 24 to 24.1 min, 1% to 70% A2; 24.1 to 28 min, 70% A2.

The ESI-MSn experiments were executed on the Thermo Q Exactive Focus mass spectrometer with the spray voltage of 3.5 kV and -2.5 kV in positive and negative modes, respectively. Sheath gas and auxiliary gas were set at 30 and 10 arbitrary units, respectively. The capillary temperature was 325°C. respectively. The Orbitrap analyzer scanned over a mass range of m/z 150 to 2000 for full scan at a mass resolution of 35000. Data dependent acquisition (DDA) MS/MS experiments were performed with HCD scan. The normalized collision energy was 30 eV. Dynamic exclusion was implemented to remove some unnecessary information in MS/MS spectra. Lipidome determination and analysis was performed by Suzhou PANOMIX Biomedical Tech Co., LTD (Jiangsu, China).

Statistical Analysis

According to the flowchart lipidome analysis was performed (Figure 1). The LipidSearch software (V4) was applied to study the lipidome profile difference between the control group and corn flour overfeeding group. Results were expressed by mean $\pm$ SD. We considered $P < 0.05$ as statistically significant. Cluster analysis, correlation analysis, principal component analysis (**PCA**), partial least squares-discriminant analysis (**PLS-DA**) and orthogonal partial least squares-discriminant analysis (**OPLS-DA**) was performed by R. The significantly different lipid was screened from the OPLS-DA model (VIP > 1.0 and $P < 0.05$). The heat map of data normalized by Z-score was generated using TBtools. Then, the Kyoto Encyclopedia of Genes and Genomes (**KEGG**) was used to search for the related KEGG pathways of the lipids. Annotation of lipid classes and species were performed as below: Glycerolipids were referred to triglyceride (**TG**), diglyceride (**DG**), monogalactosyldiacylglycerol` (**MGDG**) and monogalactosylmonoacylglycerol (**MGMG**); glycerophospholipids and lyso-glycerophospholipids were referred to phosphatidic acids (**PA**), phosphatidylinositols (**PI**), PC, PE, lysophosphatidylcholines (**LPC**); sphingolipids were referred
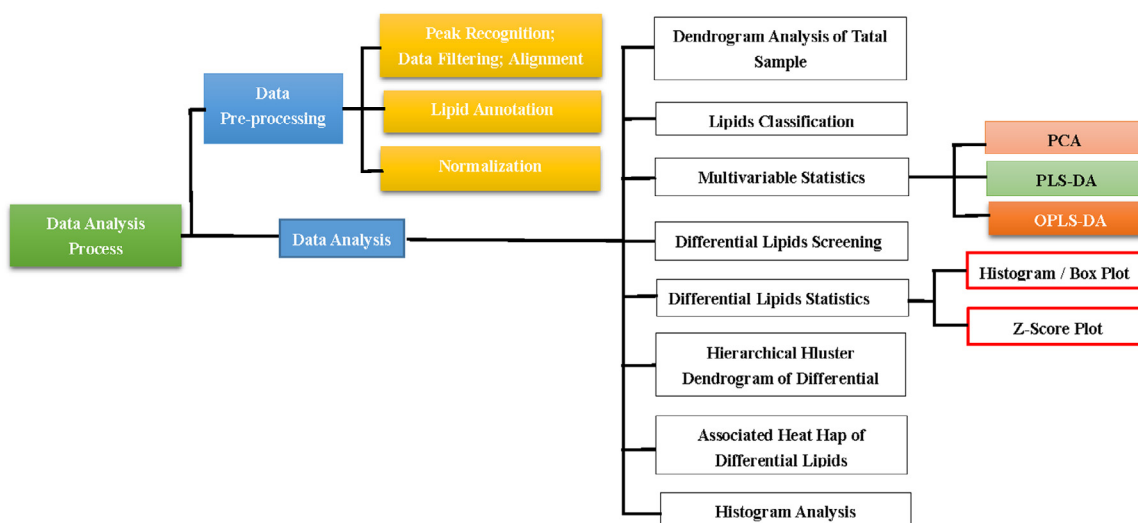

Figure 1. Goose live lipidome analysis flow diagram. OPLS-DA, orthogonal partial least squares - discriminant analysis; PCA, principal component analysis; PLS-DA, partial least squares - discriminant analysis.

to ceramides (**Cer**), hexaglycosylceramides (**Hex1Cer**) and sphingomyelins (**SM**). MetaboAnalyst5.0-pathway analysis part (https://www.metaboanalyst.ca/) was used for pathway analysis and visualization.

RESULTS

Identification of Significantly Different Lipid in Goose Liver Samples

The LipidSearch software (V4) was applied to study the lipidome profile difference between the control group and overfed group. Multivariate statistical analysis methods were implemented to analyze the lipidome data. The significantly different lipid was screened from the OPLS-DA model (VIP > 1.0 and $P < 0.05$). We observed 251 different lipids. The different lipids involved in TG, SM, PI, PE, PC, MGMG, DG, LPC, Cer, BisMePA, deMePE, MePC, and Hex1Cer categories were shown in Supplement materials 1: Figure S1-Figure S14 and in Z-score plot (Figure S15). In SM, SM, Cer and Hex1Cer elevated after overfeeding ($P < 0.05$). In PC and PE, the different lipids increased after overfeeding ($P < 0.05$). In PI, the different lipids decreased after overfeeding ($P < 0.05$); there was no significant difference between control group and corn flour overfeeding group in the PC/PE ratio (0.968 ± 0.116 vs. 1.075 ± 0.031) ($P < 0.05$). In dMePE, dMePE(18:1_20:3), dMePE(16:0_22:5), and dMePE(16:0_22:6) increased after overfeeding ($P < 0.05$). In MGDG and MGMG, MGDG(30:2e), MGDG(32:3e), MGDG(34:0e), MGDG (36:0e), MGDG(36:3), MGMG(30:0), MGMG(36:0), MGMG(37:0), MGMG(38:0), and MGMG(38:1) increased after overfeeding ($P < 0.05$). In LPC, LPC (20:4), LPC(20:5), LPC(22:4), LPC(22:5), LPC(22:6), and LPC(18:2) increased after overfeeding ($P < 0.05$). In MePC, MePC(19:4e), MePC(30:0), MePC(31:1),

MePC(32:3), MePC(33:1), MePC(33:4), MePC(34:1e), MePC(34:2), MePC(35:0e), MePC(35:1e), MePC (35:2e), MePC(35:3e), MePC(36:1), MePC(36:2e), MePC(37:0), MePC(37:0e), MePC(37:1e), MePC(37:2), MePC(37:2e), and MePC(37:5) increased after overfeeding ($P < 0.05$). In DG, DG(28:0e), DG(30:0e), DG (30:1e), DG(30:3e), DG(16:0_16:1), DG(32:1e), DG (32:3e), DG(32:4e), DG(18:0_16:0), DG(16:1_18:1), DG(18:0_18:1), and DG(18:0_20:1) decreased after overfeeding ($P < 0.05$). In TG, TG(18:0_6:0_10:0), TG (16:1_9:0_14:0), TG(16:1_9:0_16:1), TG (16:0_10:0_16:0), TG(16:0_14:0_14:0), TG (16:1_10:0_18:2), TG(11:0_16:0_18:1), TG (9:0_18:1_18:1), TG(16:0_14:1_16:0), TG (16:0_12:1_18:1), TG(16:1_14:1_16:1), TG (16:0_13:0_18:1), TG(11:0_18:1_18:1), TG (16:0_16:0_16:1), TG(16:1_16:1_17:1), TG (18:0e_16:0_16:0), TG(16:0_16:1_18:2), TG (18:0_16:0_17:0), TG(16:1_17:1_18:1), TG (18:1e_16:0_18:1), TG(16:0_18:2_18:3), TG (18:1_17:1_18:1), TG(18:1e_18:1_18:1), TG (18:0_16:0_20:5), TG(18:1_18:2_18:3), TG (18:0_18:1_19:0), and TG(20:0_18:1_18:1) increased after overfeeding ($P < 0.05$). TG(18:0e_18:1_20:1), TG (20:1_18:1_18:1), TG(18:0_18:0_20:3), TG (20:1_18:1_18:2), TG(18:0_18:0_20:4), TG (16:0_18:1_22:5), TG(18:0_19:0_20:1), TG (16:0_18:1_23:0), TG(18:1_18:1_21:0), TG (18:0_16:0_24:1), TG(16:0_18:1_24:1), TG (18:0_20:4_20:4), TG(18:0_18:1_23:0), TG (18:1_18:1_23:0), TG(18:0_18:1_24:0), TG (25:0_18:0_18:1), TG(25:0_18:1_18:1), TG (26:0_18:0_18:1), and TG(26:1_18:0_18:1) decreased after overfeeding ($P < 0.05$). Subsequently, to further investigate the distinct characteristics of the significantly different lipids, a hierarchical clustering heat map was plotted (Figure 2).
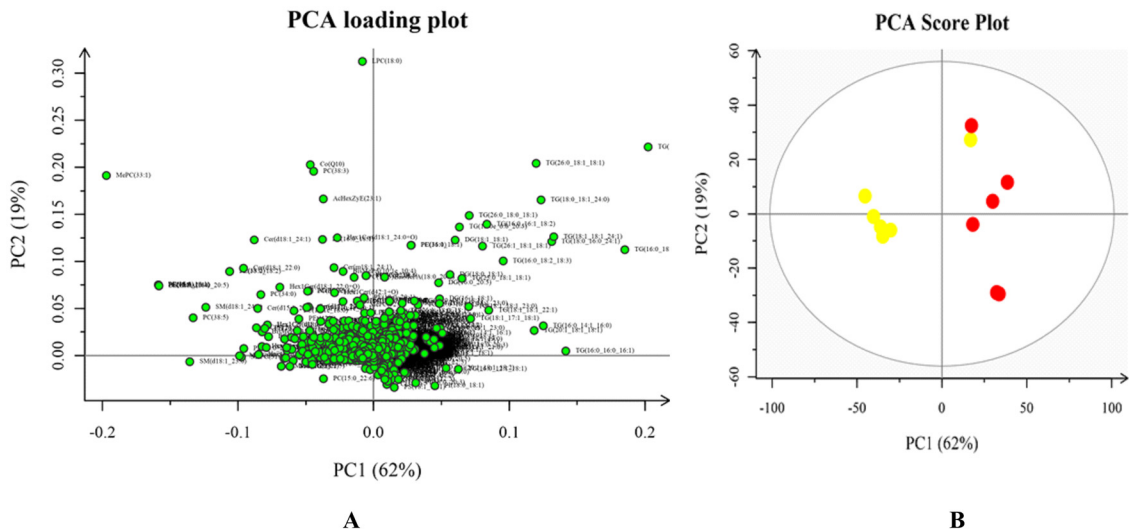

A

B

Figure 2. Hierarchical clustering analysis for the significantly different lipids (control group *vs* overfeeding group). C, control group (n = 6); Corn, corn flour overfeeding group (n = 6).

PLS-DA Score Plot

A

R2=(0.0, 0.58), Q2=(0.0, -0.02)

B

OPLS-DA Score Plot
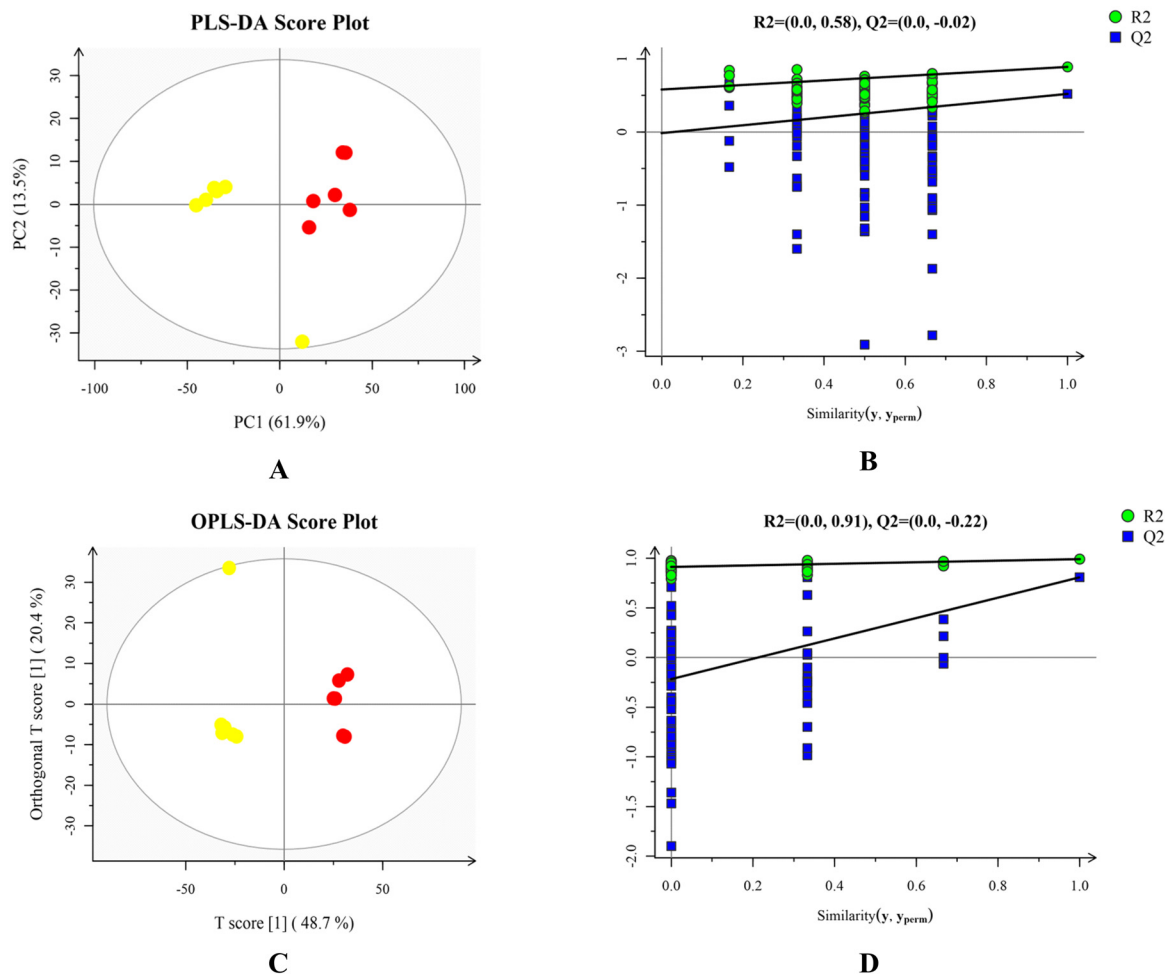
C

R2=(0.0, 0.91), Q2=(0.0, -0.22)

D

Figure 3. Lipidome profile principal component analysis (PCA). A, PCA loading plots; B, PCA score plots. Red plot represents control group (n = 6), yellow plot represents corn flour overfeeding group (n = 6).

Lipidomics Profiles Analysis of Goose Fatty Liver Formation

The comparison results of the two groups all showed obviously separation. In order to further reveal the differences in lipidomics profiles between control group and corn flour overfeeding group, PCA, PLS-DA, and OPLS-DA were performed to analyze lipidomics data. The PCA loading plots was shown in Figure 2A. The PCA score plots showed the overall changes in lipidome under the effects of overfeeding (Figure 3). In order to better understanding the classification and higher level of group separation, the PLS-DA and OPLS-DA model were used to clarify the different lipidomic patterns (Figure 4). The clear separation and discrimination were found in the PLS-DA and OPLS-DA score plot for comparison. In PLS-DA model R2Y and Q2 intercept values were 0.58 and -0.02. The low values of the Q2 Intercept represent that the robustness of the model presents a low risk of overfitting and reliability. The Q2 values are all less than 0 in our tests, thereby indicating that the PLS-DA model can identify the differences between groups and be utilized in downstream analysis (Figure 4A). Further permutation tests were performed

to validate the OPLS-DA model (R2Y = 0.91, Q2 = -0.22). In OPLS-DA score plot, the comparison results of the two groups were more obviously separated (Figure 4B). The result of PLS-DA and OPLS-DA indicated that the overall changes in lipids after overfeeding.

Different Lipids Responded to Overfeeding

The correlation analysis between different lipids was presented as a chordal graph (Figure 5) and a correlation heatmap (Supplement materials 1: Figure S-16). The line represented the Pearson correlation information of expression values among the lipids, red represents positive correlation, green represents negative correlation, and the darker the color or thicker the line represented higher correlation intensity. TG was positively correlated with DG; SM were positively associated with the Cer and Hex1Cer. DG was significantly negatively correlated with PC and PE. In order to further explore the significantly different KEGG metabolic pathways in the formation of fatty liver, the significantly different lipids were imported into KEGG database (https://
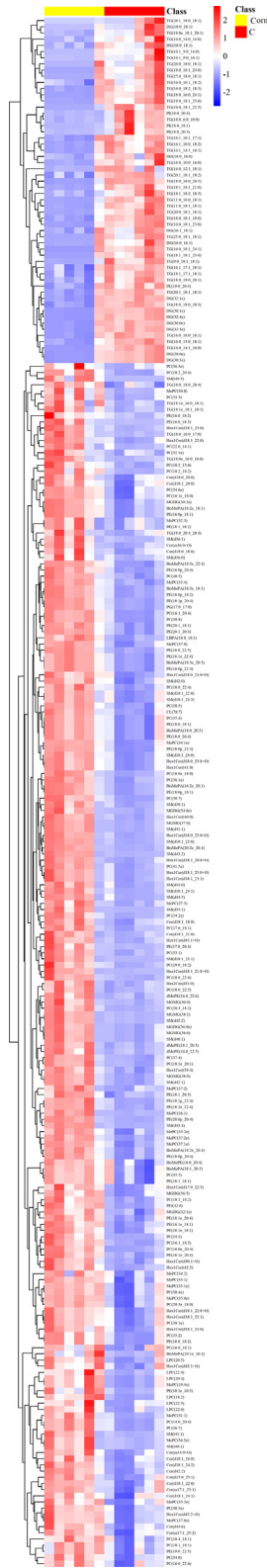
Figure 4. Lipidome profile analysis of the livers in geese for control group and corn overfeeding group. A, PLS-DA score plots; B, PLS-DA corresponding validation plots. C, OPLS-DA score plots; D, OPLS-DA corresponding validation plots. Red plot represents control group (n = 6), yellow plot represents corn flour overfeeding group (n = 6).

www.genome.jp/kegg/). After annotation, these key KEGG pathways mainly involved in Glycosylphosphatidylinositol (GPI)-anchor biosynthesis, glycerolipid metabolism, glycerophospholipid metabolism,

sphingolipid metabolism, alpha-linolenic acid metabolism, sphingolipid signaling pathway, inositol phosphate metabolism, phosphatidylinositol signaling system, linoleic acid metabolism, arachidonic acid metabolism, metabolic pathways, biosynthesis of secondary metabolites, choline metabolism in cancer, necroptosis, autophagy, tuberculosis, pathogenic escherichia coli infection, salmonella infection, kaposi sarcoma-associated herpesvirus infection, lipoarabinomannan (**LAM**) biosynthesis and retrograde endocannabinoid signaling (Supplement materials 2: Table-S2). The highest enrichment signal pathways were shown in Figure 6.

DISCUSSION

As one of the main branches of metabolomics, lipidomics aims to study lipids in body fluids, tissues and cells by various methods, explore changes in lipid metabolism under different diseases or drug interference states, and study the possible disease occurrence mechanisms and drug action from the perspective of lipid metabolic network, search for key lipid biomarkers that can characterize disease or pharmacological interventions. However, little was known if and how fat accumulation during the process of goose fatty liver formation gradually altered the liver lipidome, particularly in membrane and signaling complements. In current study, liver lipidome analysis was performed. The OPLS-DA model indicated that overfed geese liver metabolite profiles changed noticeably. Two hundred and fifty-one different lipids were yielded and were involved in TG, SM, PI, PE, PC, MGMG, DG, LPC, Cer, BisMePA, deMePE, MePC, and Hex1Cer. The significantly different lipids were enriched in these metabolic pathways in order: glycerophospholipid metabolism, glycerolipid metabolism, phosphatidylinositol signaling system, inositol phosphate metabolism, glycosylphosphatidylinositol (GPI)-anchor biosynthesis and sphingolipid metabolism.

Phospholipids are the most important component of biofilms, accounting for 40% of erythrocyte membrane lipids and 95% of mitochondrial membrane lipids, divided into glycerophospholipids and sphingolipid. PC, PE, and PI are the main glycerol phospholipids. PC is the most widely distributed and is the main component of various cell membrane structures. The PC/PE molar ratio is a determinant of cell membrane integrity and a predictor of NAFLD. Previous study had demonstrated that a decrease in the PC/PE ratio in phosphatidylethanolamine N-methyltransferase knockout mice (Pemt−/−) led to a loss of membrane integrity, followed by hepatic damage (such as ballooning) and progression to non-alcoholic steatohepatitis (**NASH**) (Li et al., 2006). In the process of goose fatty liver formation, lots of fat accumulated in hepatocytes, and hepatocytes volume increased several times. Cell membrane integrity lost, hepatocytes would burst, thus leading to liver injuries and more advanced pathological stages, for example, cirrhosis nor necrosis and even fibrosis. However, goose severe hepatic steatosis could develop without overt injury. In this study, there
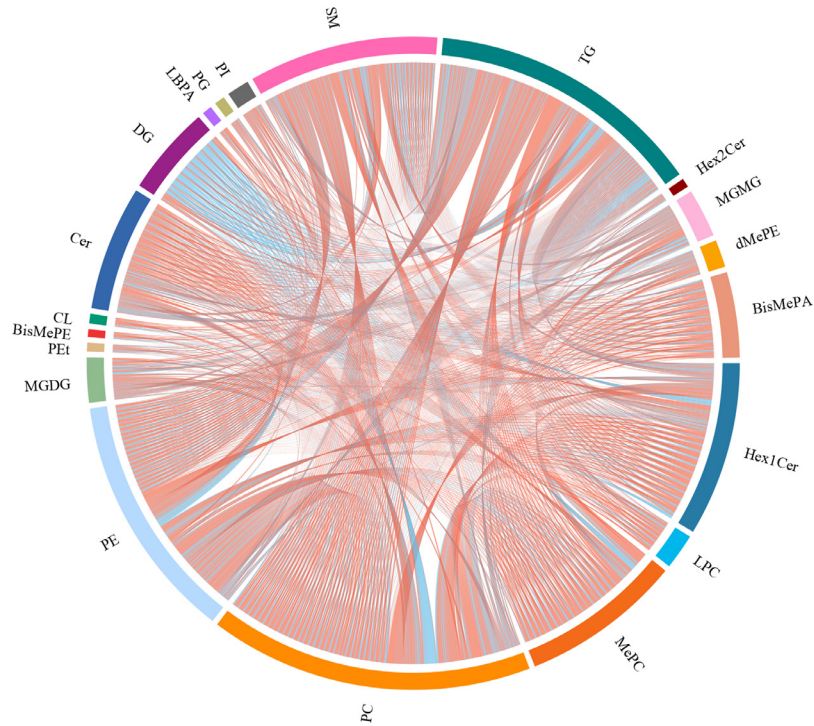
Figure 5. Correlation analysis between different lipids - chordal graph. The line represents the Pearson correlation information of expression values among the lipids, red represents positive correlation, green represents negative correlation, and the darker the color or thicker the line represents higher correlation intensity.

was no significant difference between control group and corn flour overfeeding group in the PC/PE ratio (0.968 ± 0.116 vs. 1.075 ± 0.031), which suggested that cell membrane integrity did not lose when excessive lipids deposited in liver. From the KEGG annotation results, PE mediated the autography pathway. Autophagy degrades

intracytoplasmic components in lysosomes to ensure normal cell function, which be regarded as a self-protection mechanism (Wang et al., 2019). In current study, the PE level significantly increased after overfeeding. Dysregulation of autophagy is widely involved in the pathophysiology of NAFLD. Autophagy is enhanced in the liver at
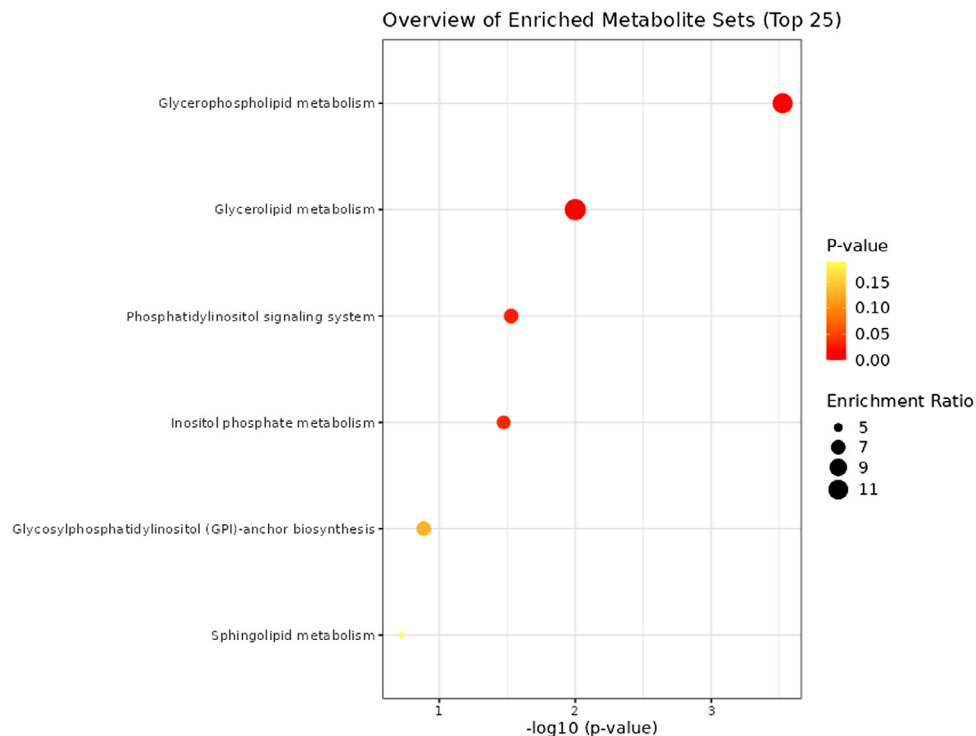

Figure 6. Lipidome view map of significant metabolic pathways − enrichment analysis. This view map was generated from MetaboAnalyst5.0.

the early stage of NAFLD, and is gradually inhibited as the disease progresses to the later stage. The results of autophagy flux analysis also showed that autophagic synthesis and degradation occurred in the early stage and were gradually inhibited afterwards (Ding et al., 2020). LPC can be used as a potential biomarker for the risk of developing liver disease, and low LPC level indicated inflammatory and oxidative stress (Wang et al., 2017). In current study, LPC(20:4), LPC(20:5), LPC(22:4), LPC (22:5), LPC(22:6), and LPC(18:2) significantly increased after overfeeding. LPC (20:4) induced Fas and TNFα pathways, resulting in apoptosis and thus playing a tumor suppressive role (Paul et al., 2022). As said above, the changes of liver phospholipids responded to overfeeding contributed to shape the goose liver tolerance to severe hepatic steatosis.

Sphingolipids are the main structural components of lipid bilayer of cell membrane and regulate important physiological functions of cells. Sphingomyelin consists of sphingosine, fatty acids, phosphate group and nitrogenous bases. *De novo* synthesis of sphingosine starts with the synthesis of Cer. Thereby, intracellular sphingolipid metabolism is centered on Cer, which is the production and breakdown of Cer and the synthesis of complex sphingolipids from Cer (Choi et al., 2021). Overfeeding increased the levels of SM, Cer, and Hex1Cer, which partially reflected the relationship between SM, Cer, and Hex1Cer. The base in sphingomyelin is usually choline, formed from Cer and phosphatidylcholine. The reaction is catalyzed by sphingomyelin synthase. Sphingomyelinase catalyzes sphingomyelin degradation to Cer and phosphocholine (Hannun and Obeid, 2018). Therefore, sphingomyelin is not only an important membrane phospholipid, but also a Cer reservoir. Their metabolic abnormalities are closely related to a variety of chronic diseases. In this current study, the levels of SM, Cer, and Hex1Cer were increased after overfeeding, which was consistent with previous report that sphingolipid metabolism disorders were characterized by sphingolipids elevation such as Cer in tissue accumulation and circulation (Chaurasia and Summers, 2021). In addition, increased lipids included Cer in both the blood and livers of NAFLD patients (Gorden et al., 2015), as well as dihydroceramides which are basic markers of de novo Cer synthesis (Apostolopoulou et al., 2018). As such, murine models had shown that hepatic steatosis decreased when levels of liver Cer were lowered by deletion of dihydroceramide desaturase or increasing acid ceramidase activity (Xia et al., 2015). Many cellular stress inducers, such as inflammation activation, excess saturated fatty acid intake, and chemotherapy, have been shown to increase ceramide synthesis rates. Current study showed that overfeeding elevated the liver Cer levels. As said above, the capacity for and the tolerance to severe hepatic steatosis without overt liver injuries in overfed goose. These findings suggested that existence of protective mechanism contributed to the inhibition of inflammation induced by Cer in goose fatty liver. Adiponectin can activate ceramidase and promote ceramide degradation. Adiponectin levels are significantly decreased in obesity and related pathological states (Reibe-Pal and Febbraio, 2017). However, the mRNA levels of adiponectin receptors1/2 (Adipor1/2) were increased in overfeeding-induced fatty livers of geese (Geng et al., 2016a).

Glycerolipids are referred to TG and DG. After overfeeding, the geese or duck received high energy, as a result of which the substrates for fatty acid synthesis (glucose) increased substantially in the liver. Meanwhile, the content of TG produced far exceeded the transport capacity of apolipoproteins, and the fatty acid produced far exceeded the degraded fatty acid by β-oxidation, thus leading to the accumulation of lipids in the liver (Wei et al., 2020). In current study, overfeeding increased liver TG level, which consisted with the liver weight and liver slice results reported by previous study (Wei et al., 2022a). DG and inositol phosphate are the second messenger in phosphoinositol signaling pathway. DG activates protein kinase C (**PKC**), and activated PKC causes the substrate phosphorylation to trigger a cellular response; 1,4, 5-triphosphate inositol (**IP3**) induces cellular responses by mobilizing intracellular calcium into the cytoplasmic matrix and elevating cytoplasmic free Ca^{2+} concentrations; (Shi et al., 2019). PI3K/Akt pathway is the classical phosphoinositol signaling pathway. Fork head transcription factor 1 (FoxO1), a major target of Akt, is a transcription factor negatively regulated by insulin signaling. Our previous researches had confirmed that PI3K/Akt/mTOR pathway regulated cell proliferation and lipid metabolism via mediating insulin signaling pathway and FoxO1 in goose primary hepatocytes (Han et al., 2015; Han et al., 2016; Liu et al., 2016a; Wei et al., 2022b). Akt directly inhibited FoxO1 and reduced glucose levels in serum (Yang et al., 2018). Activation of Akt inhibited mTORC1 to reduce lipid and protein production (Kenerson et al., 2011). Increased DG levels induced by excessive FFA oxidation cut off the PI3K/Akt pathway and exacerbated IR in liver (Khan et al., 2019). In current study, the levels of DG and PI decreased after overfeeding, which may help us to understand a fact that IR was not observed in waterfowl (Davail et al., 2003; Gontier et al., 2013; Geng et al., 2015; Pioche et al., 2020).

CONCLUSION

In summary, this is the first report describing the goose fatty liver formation from lipidomics. Lipidome change responded to overfeeding, and significantly different lipids and metabolic pathways were identified during the formation of goose fatty liver. Different lipids cooperatively promoted the formation of fatty liver during overfeeding, the different lipids jointly shaped the goose liver capacity for and tolerance to severe hepatic steatosis. Although, the interaction between different lipids and metabolic pathways needs further verified, our present work could provide a relatively comprehensive lipidomics landscape for goose fatty liver formation mechanism.

ACKNOWLEDGMENTS

DISCLOSURES

We declare that all authors have no conflict of interest about this manuscript.

SUPPLEMENTARY MATERIALS

Supplementary material associated with this article can be found, in the online version, at doi:10.1016/j. psj.2022.102428.

REFERENCES

Akerele, O. A., and S. K. Cheema. 2015. Fatty acyl composition of lysophosphatidylcholine is important in atherosclerosis. Med. Hypotheses 85:754–760.

Apostolopoulou, M., R. Gordillo, C. Koliaki, S. Gancheva, T. Jelenik, E. De Filippo, C. Herder, D. Markgraf, F. Jankowiak, I. Esposito, M. Schlensak, P. E. Scherer, and M. Roden. 2018. Specific hepatic sphingolipids relate to insulin resistance, oxidative stress, and inflammation in nonalcoholic steatohepatitis. Diabetes Care 41:1235–1243.

Chaurasia, B., and S. A. Summers. 2021. Ceramides in metabolism: key lipotoxic players. Pages 303-330 in Annual Review of Physiology, Vol 83. M. T. Nelson, and K. Walsh eds.

Choi, R. H., S. M. Tatum, J. D. Symons, S. A. Summers, and W. L. Holland. 2021. Ceramides and other sphingolipids as drivers of cardiovascular disease. Nat. Rev. Cardiol. 18:701–711.

Davail, S., G. Guy, J. Andre, D. Hermier, and R. Hoo-Paris. 2000. Metabolism in two breeds of geese with moderate or large overfeeding induced liver-steatosis. Comp. Biochem. Physiol. A Mol. Integr. Physiol. 126:91–99.

Davail, S., N. Rideau, G. Guy, J. M. Andre, and R. Hoo-Paris. 2003. Pancreatic hormonal and metabolic responses in overfed ducks. Hormone Metab. Res. Hormon- Stoffwechselforschung Hormones et metabolisme 35:439–443.

Ding, H., G. Ge, Y. Tseng, Y. Ma, J. Zhang, and J. Liu. 2020. Hepatic autophagy fluctuates during the development of non-alcoholic fatty liver disease. Ann. Hepatol. 19:516–522.

Geng, T., B. Yang, F. Li, L. Xia, Q. Wang, X. Zhao, and D. Gong. 2016a. Identification of protective components that prevent the exacerbation of goose fatty liver: Characterization, expression and regulation of adiponectin receptors. Comp. Biochem. Physiol. B Biochem. Mol. Biol. 194-195:32–38.

Geng, T., X. Zhao, L. Xia, L. Liu, F. Li, B. Yang, Q. Wang, S. Montgomery, H. Cui, and D. Gong. 2016b. Supplementing dietary sugar promotes endoplasmic reticulum stress-independent insulin resistance and fatty liver in goose. Biochem. Biophys. Res. Commun. 476:665–669.

Geng, T., Y., L. L. Xia, F. Y. Li, J. Xia, Y. H. Zhang, Q. Q. Wang, B. Yang, S. Montgomery, H. M. Cui, and D. Q. Gong. 2015. The role of endoplasmic reticulum stress and insulin resistance in the occurrence of goose fatty liver. Biochem. Biophys. Res. Commun. 465:83–87.

Gontier, K., J.-M. Andre, M.-D. Bernadet, K. Ricaud, and S. Davail. 2013. Insulin effect on lipogenesis and fat distribution in three genotypes of ducks during overfeeding. Comp. Biochem. PhysiolMol. Integrat. Physiol. 164:499–505.

Gorden, D. L., D. S. Myers, P. T. Ivanova, E. Fahy, M. R. Maurya, S. Gupta, J. Min, N. J. Spann, J. G. McDonald, S. L. Kelly, J. Duan, M. C. Sullards, T. J. Leiker, R. M. Barkley, O. Quehenberger, A. M. Armando, S. B. Milne, T. P. Mathews, M. D. Armstrong, C. Li, W. V. Melvin, R. H. Clements,

M. K. Washington, A. M. Mendonsa, J. L. Witztum, Z. Guan, C. K. Glass, R. C. Murphy, E. A. Dennis, A. H. Merrill Jr, D. W. Russell, S. Subramaniam, and H. A. Brown. 2015. Biomarkers of NAFLD progression: a lipidomics approach to an epidemic. J. Lipid Res. 56:722–736.

Han, C., S. Wei, F. He, D. Liu, H. Wan, H. Liu, L. Li, H. Xu, X. Du, and F. Xu. 2015. The regulation of lipid deposition by insulin in goose liver cells is mediated by the PI3K-AKT-mTOR signaling pathway. PLoS One 10:e0098759, doi:10.1371/journal.pone.0098759..

Han, C., S. Wei, Q. Song, F. He, X. Xiong, H. Wan, D. Liu, F. Ye, H. Liu, L. Li, H. Xu, X. Du, B. Kang, and X. Zeng. 2016. Insulin stimulates goose liver cell growth by activating PI3K-AKT-mTOR signal pathway. Cell. Physiol. Biochem. 38:558–570.

Hannun, Y. A., and L. M. Obeid. 2018. Sphingolipids and their metabolism in physiology and disease. Nat. Rev. Mol. Cell Biol. 19:175–191.

Kenerson, H. L., M. M. Yeh, and R. S. Yeung. 2011. Tuberous sclerosis complex-1 deficiency attenuates diet-induced hepatic lipid accumulation. PLoS One 6:e18075, doi:10.1371/journal.pone.0018075..

Khan, R. S., F. Bril, K. Cusi, and P. N. Newsome. 2019. Modulation of insulin resistance in nonalcoholic fatty liver disease. Hepatology 70:711–724.

Li, Z., L. B. Agellon, T. M. Allen, M. Umeda, L. Jewell, A. Mason, and D. E. Vance. 2006. The ratio of phosphatidylcholine to phosphatidylethanolamine influences membrane integrity and steatohepatitis. Cell Metab. 3:321–331.

Liu, D. D., C. C. Han, H. F. Wan, F. He, H. Y. Xu, S. H. Wei, X. H. Du, and F. Xu. 2016a. Effects of inhibiting PI3K-Akt-mTOR pathway on lipid metabolism homeostasis in goose primary hepatocytes. Animal 10:1319–1327.

Liu, L., X. Zhao, Q. Wang, X. X. Sun, L. L. Xia, Q. Q. Wang, B. Yang, Y. H. Zhang, S. Montgomery, H. Meng, T. Y. Geng, and D. Q. Gong. 2016b. Prosteatotic and protective components in a unique model of fatty liver: gut microbiota and suppressed complement system. Sci. Rep. 6.

Lu, L., Y. Chen, Z. Wang, X. Li, W. Chen, Z. Tao, J. Shen, Y. Tian, D. Wang, G. Li, L. Chen, F. Chen, D. Fang, L. Yu, Y. Sun, Y. Ma, J. Li, and J. Wang. 2015. The goose genome sequence leads to insights into the evolution of waterfowl and susceptibility to fatty liver. Genome Biol. 16:89.

Paul, B., M. Lewinska, and J. B. Andersen. 2022. Lipid alterations in chronic liver disease and liver cancer. Jhep Rep. 4:100479, doi:10.1016/j.jhepr.2022.100479.

Pioche, T., F. Skiba, M.-D. Bernadet, I. Seiliez, W. Massimino, M. Houssier, A. Tavernier, K. Ricaud, S. Davail, S. Skiba-Cassy, and K. Gontier. 2020. Kinetic study of the expression of genes related to hepatic steatosis, glucose and lipid metabolism, and cellular stress during overfeeding in mule ducks. Am. J. Physiol-Regulat Integrat. Com. Physiol. 318:R453–R467.

Reibe-Pal, S., and M. A. Febbraio. 2017. Adiponectin serenades ceramidase to improve metabolism. Mol. Metab. 6:233–235.

Shi, X., J. Wang, Y. Lei, C. Cong, D. Tan, and X. Zhou. 2019. Research progress on the PI3K/AKT signaling pathway in gynecological cancer (Review). Mol. Med. Rep. 19:4529–4535.

Song, H., X. Feng, H. Zhang, Y. Luo, J. Huang, M. Lin, J. Jin, X. Ding, S. Wu, H. Huang, T. Yu, M. Zhang, H. Hong, S. Yao, Y. Zhao, and Z. Zhang. 2019. METTL3 and ALKBH5 oppositely regulate m(6)A modification of TFEB mRNA, which dictates the fate of hypoxia/reoxygenation-treated cardiomyocytes. Autophagy 15:1419–1437.

Vvedenskaya, O., T. D. Rose, O. Knittelfelder, A. Palladini, J. A. H. Wodke, K. Schuhmann, J. M. Ackerman, Y. Wang, C. Has, M. Brosch, V. R. Thangapandi, S. Buch, T. Zuellig, J. Hartler, H. C. Koefeler, C. Roecken, U. Coskun, E. Klipp, W. von Schoenfels, J. Gross, C. Schafmayer, J. Hampe, J. K. Pauling, and A. Shevchenko. 2021. Nonalcoholic fatty liver disease stratification by liver lipidomics. J. Lipid Res. 62:100104, doi:10.1016/j.jlr.2021.100104..

Wang, F., Y. Wang, G. Qu, Y. Yao, C. Ma, M. Song, H. Wang, and G. Jiang. 2019. Ultralong AgNWs-induced toxicity in A549 cells and the important roles of It ROS and autophagy. Ecotoxicol. Environ. Saf. 186:109742, doi:doi.10.1016/j.ecoenv.2019.109742.

Wang, X.-F., W.-Y. Wu, G.-K. Qiu, H. Wang, W.-S. Li, Y.-L. Wang,

Q.-Q. Jiang, M.-F. Han, and Q. Ning. 2017. Plasma lipidomics identifies novel biomarkers in patients with hepatitis B virus-related acute-on-chronic liver failure. Metabolomics 13:76, doi: doi.10.1007/s11306-017-1215-x.

Wei, R., D. Deng, Y. Teng, C. Lu, Z. Luo, M. Abdulai, H. Liu, H. Xu, L. Li, S. Hu, J. Hu, S. Wei, X. Zeng, and C. Han. 2022a. Study on the effect of different types of sugar on lipid deposition in goose fatty liver. Poult. Sci. 101:101729 -101729.

Wei, R., C. Han, D. Deng, F. Ye, X. Gan, H. Liu, L. Li, H. Xu, and S. Wei. 2020. Research progress into the physiological changes in metabolic pathways in waterfowl with hepatic steatosis. Br. Poult. Sci. 62:118–124.

Wei, R., C. Han, F. Ye, S. Wei, F. He, H. Liu, L. Li, H. Xu, S. Hu, and X. Zeng. 2022b. Forkhead box protein O1 (FoxO1) regulates lipids metabolism and cell proliferation mediated by insulin and PI3K-Akt-mTOR pathway in goose primary hepatocytes. Biocell 46:171–183.

Xia, J. Y., W. L. Holland, C. M. Kusminski, K. Sun, A. X. Sharma, M. J. Pearson, A. J. Sifuentes, J. G. McDonald, R. Gordillo, and P. E. Scherer. 2015. Targeted induction of ceramide degradation leads to improved systemic metabolism and reduced hepatic steatosis. Cell Metab. 22:266–278.

Xia, L., Q. Wang, B. Yang, X. Sun, Y. Zhang, L. Liu, Y. Geng, and D. Gong. 2016. Study on change of blood chemistry indexes, hepatic routine nutritional composition and expression of lipid metabolism-associatd genes during the recovery of geese with fatty. China An. Husband. Med. 43:967–972.

Yang, S.-Q., Y.-D. Chen, H. Li, X. Hui, and W.-Y. Gao. 2018. Geniposide and gentiopicroside suppress hepatic gluconeogenesis via regulation of AKT-FOXO1 pathway. Arch. Med. Res. 49:314–322.

Zhu, Q., H. Li, Z. Ao, H. Xu, J. Luo, C. Kaurich, R. Yang, P.-W. Zhu, S.-D. Chen, X.-D. Wang, L.-J. Tang, G. Li, O.-Y. Huang, M.-H. Zheng, H.-P. Li, and F. Liu. 2022. Lipidomic identification of urinary extracellular vesicles for non-alcoholic steatohepatitis diagnosis. J. Nanobiotechnol. 20:349, doi:doi.10.1186/s12951-022-01540-4..